analytical chemistry

Article

pubs.acs.org/ac

Polydimethylsiloxane-Paper Hybrid Lateral Flow Assay for Highly Sensitive Point-of-Care Nucleic Acid Testing

Jane Ru Choi,[†,‡,§] Zhi Liu,[§,∥] Jie Hu,[†,§] Ruihua Tang,[†,§,⊥,#] Yan Gong,[†,§] Shangsheng Feng,[§,¶,∇] Hui Ren,[§,○] Ting Wen,[◆] Hui Yang,[⊥,#] Zhiguo Qu,[∥] Belinda Pingguan-Murphy,[‡] and Feng Xu*[,†,§]

[†]The Key Laboratory of Biomedical Information Engineering of Ministry of Education, School of Life Science and Technology, Xi'an Jiaotong University, Xi'an, Shaanxi 710049, PR China

[‡]Department of Biomedical Engineering, Faculty of Engineering, University of Malaya, Lembah Pantai, 50603 Kuala Lumpur, Malaysia

[§]Bioinspired Engineering and Biomechanics Center (BEBC), Xi'an Jiaotong University, Xi'an, Shaanxi 710049, PR China

[∥]Key Laboratory of Thermo-Fluid Science and Engineering of Ministry of Education, School of Energy and Power Engineering, Xi'an Jiaotong University, Xi'an, Shaanxi 710049, PR China

[⊥]School of Life Sciences, Northwestern Polytechnical University, Xi'an, Shaanxi 710072, PR China

[#]Key Laboratory of Space Bioscience and Biotechnology, Northwestern Polytechnical University, Xi'an, Shaanxi 710072, PR China

[¶]MOE Key Laboratory of Multifunctional Materials and Structures (LMMS), School of Aerospace, Xi'an Jiaotong University, Xi'an, Shaanxi 710049, PR China

[∇]State Key Laboratory of Mechanical Structure Strength and Vibration, School of Aerospace, Xi'an Jiaotong University, Xi'an, Shaanxi 710049, PR China

[○]Department of Respiratory and Critical Care Medicine, The First Affiliated Hospital of Xi'an Jiaotong University, Xi'an, Shaanxi 710061, PR China

[◆]Xi'an Diandi Biotech Company, Xi'an, Shaanxi 710049, PR China

Supporting Information

ABSTRACT: In nucleic acid testing (NAT), gold nanoparticle (AuNP)-based lateral flow assays (LFAs) have received significant attention due to their cost-effectiveness, rapidity, and the ability to produce a simple colorimetric readout. However, the poor sensitivity of AuNP-based LFAs limits its widespread applications. Even though various efforts have been made to improve the assay sensitivity, most methods are inappropriate for integration into LFA for sample-to-answer NAT at the point-of-care (POC), usually due to the complicated fabrication processes or incompatible chemicals used. To address this, we propose a novel strategy of integrating a simple fluidic control strategy into LFA. The strategy involves incorporating a piece of paper-based shunt and a polydimethylsiloxane (PDMS) barrier to the strip to achieve optimum fluidic delays for LFA signal enhancement, resulting in 10-fold signal enhancement over unmodified LFA. The phenomena of fluidic delay were also evaluated by mathematical simulation, through which we found the movement of fluid throughout the shunt and the tortuosity effects in the presence of PDMS barrier, which significantly affect the detection sensitivity. To demonstrate the potential of integrating this strategy into a LFA with sample-in-answer-out capability, we further applied this strategy into our prototype sample-to-answer LFA to sensitively detect the Hepatitis B virus (HBV) in clinical blood samples. The proposed strategy offers great potential for highly sensitive detection of various targets for wide application in the near future.

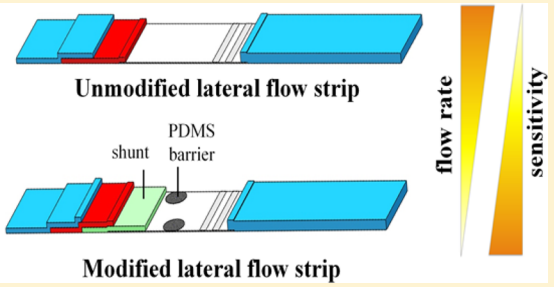

Nucleic acid testing (NAT) plays a fundamental role in medical diagnostic applications, food safety analysis, and environmental monitoring.[1−3] Conventional NAT normally involves labor-intensive and time-consuming processes (e.g., phenol-chloroform-based extraction, polymerase chain reaction (PCR), and electrophoresis) and sophisticated and expensive equipment (e.g., thermal cycler, centrifuge machine, electrophoresis unit, and gel documentation system), which are generally limited to the central laboratory.[4−6] In recent studies, gold nanoparticle (AuNP)-based lateral flow assays (LFAs) have been demonstrated as a potential diagnostic tool for NAT, especially in amplicon detection with simple colorimetric readout, which offers great capability of rapid diagnosis at the

Received: January 16, 2016
Accepted: March 24, 2016
Published: March 25, 2016

DOI: 10.1021/acs.analchem.6b00195
Anal. Chem. 2016, 88, 6254−6264

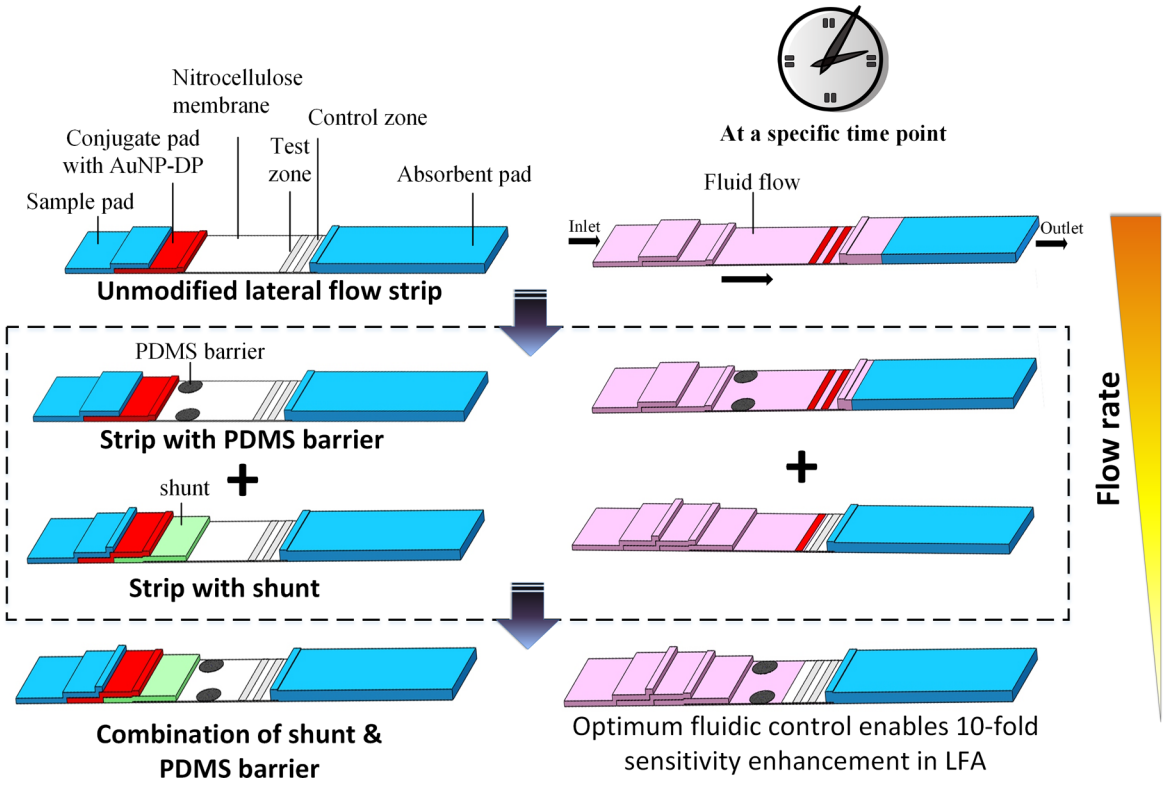

Figure 1. Schematic diagram showing the strategy of fluidic delays in LFA. The combination of shunt and PDMS barriers in LFA shows significant fluidic delays as compared to LFA with shunt or PDMS barrier alone and unmodified LFA. This strategy enables 10-fold signal enhancement in LFA as compared to the unmodified LFA, showing great potential to sensitively detect various targets at the point of care.

point of care (POC).[7−9] In the presence of biotinylated amplicon (DNA), the DNA would bind to the gold nanoparticle-detector probe (AuNP-DP) on the conjugate pad and form AuNP-DP-DNA conjugate. The conjugate would then migrate along the paper strip via capillary force and bind to the streptavidin at the test zone to form a visible red signal. The excess AuNP-DP would be captured by the control probe at the control zone, producing a red signal for assay validation.[10,11]

In fact, the poor sensitivity of AuNP-based LFAs limits its widespread application.[12] To this end, significant efforts have been made to improve their sensitivity using various approaches such as enzyme-based signal enhancement,[13] probe-based signal enhancement,[14] sample concentration,[15,16] and thermal contrast.[17] However, these techniques require special design of DNA sequences,[14] external electrical power sources,[15,17] or multiple operation steps,[13,16] limiting their use for POC testing. In contrast, fluidic control in LFA could significantly improve the sensitivity of the assay with simple strip fabrication and operation steps, which have currently attracted significant research interest.[18,19]

Several studies have reported various methods of controlling fluid flow and reagent transport in LFA by creating wax barriers[18,20] or alteration of the geometry of the paper network.[19] Despite their potential of improving the analytical sensitivity of an assay through fluidic delays, most of these methods are less suitable to be integrated into LFAs with sample-in-answer-out capabilities (i.e., integrated extraction, amplification, and colorimetric detection) due to several reasons. Importantly, to develop a miniaturized sample-to-answer lateral flow strip for rapid NAT which involves the aforementioned three main steps, a heat-dependent amplification process is normally required prior to detection.[21] In this context, a wax barrier on the strip may melt during the heating process,[22] hence affecting the fluidic control strategy. On the other hand, increasing the fluidic path length or width or sample pad modification as suggested by the existing study[19] makes the total size of the strip larger and consumes a higher volume of reagent and sample, which undermines the unique advantages of POC use. In addition, the irregular size of such a biosensor makes the manufacturing process more complicated. Therefore, to meet the increasing need for portable, rapid, robust, inexpensive, easily performable, and importantly, highly sensitive NAT for POC testing, integrating a simple fluidic control strategy into a sample-to-answer LFA without involving incompatible chemical is highly desirable.

In the present study, we demonstrate a novel strategy of incorporating a paper-based shunt and a polydimethylsiloxane (PDMS) barrier into the strip. PDMS was selected, because it is inexpensive, inert, nontoxic, and (unlike wax suggested by the existing studies[18,20]) heat-resistant,[23] complementing the heating process normally required for sample-to-answer NAT. Interestingly, we found that creating a PDMS barrier alone would not sufficiently enhance the signal whereas implementing a larger shunt alone would be sample-consuming. This motivates us to integrate both an optimum size of shunt and an optimum amount of PDMS droplets into LFA to control the fluid transport, achieving an optimum fluidic delay for analytical sensitivity enhancement without consuming a large volume of sample. The phenomena of fluidic delays were evaluated by mathematical simulation, through which we found the fluid movement throughout the shunt and the effect of tortuosity in the presence of PDMS, which significantly affect the detection sensitivity. With this strategy, optimum recognition between

DOI: 10.1021/acs.analchem.6b00195
Anal. Chem. 2016, 88, 6254−6264

the target analyte and AuNP-DP is achieved, increasing the binding efficiency between the capturing molecule and the AuNP-DP-target in a desirable time period. The fluidic control strategy allows highly sensitive medical diagnosis, yielding a 10-fold signal enhancement over conventional unmodified LFA. This strategy was applied to our previously developed LFA,[24] involving paper-based extraction, amplification, and lateral flow detection, to sensitively detect Hepatitis B virus (HBV) in clinical blood samples. The developed LFA shows great promise to sensitively detect various targets for a wide range of applications including biomedical diagnosis, food safety control, and environmental monitoring.

EXPERIMENTAL SECTION

Preparation of AuNP and DP Conjugates. AuNPs with a diameter of 13 ± 3 nm and AuNP-DP conjugates were prepared according to the previous published protocol.[12] The AuNP-DP conjugates have been characterized by visible color changes from wine red to dark red, aggregate formation in transmission electron microscopy (TEM), and a slight shift of the absorbance values (6 nm) in ultraviolet−visible (UV/vis) spectrophotometry.[25]

Preparation of Lateral Flow Strip Implemented with Shunt, PDMS Droplets, and the Combination of Both. The synthetic DNA used in the optimization assay was Hepatitis B viral DNA with the sequences obtained from the Sangon Biotechnology Co., Ltd. (Shanghai, China) (Supplementary Table 1). The unmodified lateral flow test strip is composed of a nitrocellulose membrane (30 cm × 2.0 cm × 0.01 cm) (HFB 18002, Millipore, USA), a sample pad (30 cm × 1.2 cm × 0.05 cm) (Pall 8964, Saint Germain-en-Laye, France), a conjugate pad (30 cm × 1 cm × 0.05 cm) (Pall 8964, Saint Germain-en-Laye, France), an absorbent pad (30 cm × 2.5 cm × 0.1 cm) (H-1, Jiening, China), and a PVC backing pad (30 cm × 6.0 cm × 0.02 cm) (J-B6, Jiening, China). The assembled pad was cut into a large number of strips with 0.25 cm width and 6 cm length using a Matrix 2360 Programmable Shear.

To demonstrate the potential of implementing a shunt into LFA for fluidic delay to enhance the assay sensitivity, test strips with different lengths of shunt (0.5, 0.75, 1, 1.25, and 1.5 cm) were prepared. The width of shunt was maintained the same as that of the test strip to keep the fabrication process simple. The shunt was placed between the conjugate pad (glass fiber) and the nitrocellulose membrane, with a 0.5 cm × 0.25 cm overlapping region between the two conjugate pads, and also between the conjugate pad and the shunt (Figure 1). The surface area of the overlapping region between the conjugate pad and the nitrocellulose membrane was 0.1 cm × 0.25 cm in unmodified lateral flow strip, which was similar to that between the nitrocellulose membrane and the absorbent pad of all test strips.

To evaluate the possibility of incorporating PDMS droplets into LFA for sensitivity improvement, we added different numbers of PDMS droplets (one, two, three, four, and five droplets) onto the nitrocellulose membrane by using a pipet. The volume of each PDMS droplet was 0.1 μL, and the distance between each droplet was maintained at 2 mm. Following the dispension of the droplets onto the nitrocellulose membrane, the test strips were dried in an oven at 37 °C for about 1 h. Thereafter, to further improve the sensitivity of LFA with optimum fluidic control, we incorporated both shunt and PDMS droplets into the lateral flow strip. The optimum length of shunt was combined with 1, 2 or a maximum of 3 droplets of PDMS to achieve optimum sensitivity of the assay.

About 0.5 μL of 100 μM control probe and 0.5 μL of 2 mg/mL streptavidin were dispensed on control zone and test zone, respectively, which are based on the optimization result from our group.[12,26] All test strips were dried in the oven at 37 °C. After the drying, 50 μL of saline sodium citrate (SSC) buffer (4× , pH 7.0) was added into a 96-well plate. LFA was performed by immersing the test strip into the well plate until the test zone and control zone turn red. At the end of the assay, images of all test zones were captured with a smartphone and the color intensities were then converted to optical density with an APP developed by our group. All tests were performed at room temperature (25 °C).

Mathematical Simulation. To mathematically simulate the phenomena of liquid flow in LFA, a 3D physical model for a steady-state flow in a fluid-saturated strip (as heterogeneous porous medium) was presented in this study. The flow can be described by the Brinkman equation for the porous regions, in which the viscosity effect is taken into consideration:

$$\nabla p = -\frac{\mu}{K}\vec{V} + \mu_e \nabla^2 \vec{V} \tag{1}$$

where $\vec{V}$, p, μ, μ_e, and K are fluid velocity, pressure, fluid viscosity, effective viscosity for Brinkman term, and permeability of porous medium, respectively. The fluid viscosity (μ) is approximate to that of the water at 20 °C. The effective viscosity (μ_e) is assumed to correspond to the fluid viscosity (μ) in thin porous layers.[27] The permeability K for different types of porous materials was evaluated by the selected empirical equations. For random overlapping fiber porous materials, such as the glass fiber and the absorbent pad in our LFA, the empirical equation of the permeability K is given as follows:[28]

$$K = r^2 \frac{\pi\varepsilon(1 - \sqrt{1 - \varepsilon})^2}{24(1 - \varepsilon)^{1.5}} \tag{2}$$

where ε is material porosity and r is the average fiber radius in fiber porous material. As for the granular porous material, in this case, nitrocellulose membrane, permeability K was obtained through the Kozeny-Carman equation:[29]

$$K = \frac{d^2\varepsilon^3}{180(1 - \varepsilon)^2} \tag{3}$$

where d is average pore diameter. The porosity ε was obtained by the empirical method through measuring the volume of liquid absorbed by the materials.[30] Both the average fiber radius r and average pore diameter d were obtained from the scanning electron microscopy (SEM) figures of the material (data not shown).

As shown in Figure 1, the boundary conditions are summarized as follows. The inlet velocity was calculated with the known sample volume (100 μL), the inlet cross-section, and the period required for fluid absorption. The pressure at the outlet is equal to the atmospheric pressure. All other bounding walls are under nonslip conditions. The mathematical simulation was done using the Brinkman equation module of Comsol Multiphysics 5.0 software.

Fabrication of an Integrated Paper-Based Sample-to-Answer LFA. Briefly, the integrated paper-based sample-to-answer LFA consists of 4 layers. The top PVC layer is a lateral flow layer, and the second layer is an amplification layer which

DOI: 10.1021/acs.analchem.6b00195
Anal. Chem. 2016, 88, 6254−6264

consists of a glass fiber for loop-mediated isothermal amplification (LAMP). The third layer is an extraction layer, which consists of a FTA card (Whatman, UK), with a diameter of 0.25 cm, for sample addition and nucleic acid extraction. The bottom layer is a cellulose layer to absorb the waste produced by the process of sample purification and washing. All materials were assembled to create an integrated paper-based sample-to-answer LFA. A piece of 3.5 cm × 2 cm adhesive tape was folded in half, creating a small pocket that acts as a reaction chamber for LAMP, into which both glass fiber and FTA card were inserted, to prevent sample evaporation.

Paper-Based Extraction, Amplification, and Lateral Flow Detection Using the Integrated Sample-to-Answer LFA. The process of paper-based extraction, amplification, and detection were performed by using the integrated LFA coupling with a specially designed hand-held battery powered heating device according to our previously published protocol.[31] Briefly, the HBV blood sample was added onto the FTA card that is impregnated with chemicals to lyse the cells at room temperature. Following the cell lysis, a purification and washing step is required to remove all the sample waste (e.g., cell debris, protein, and other components) and the chemicals, which may affect the downstream analysis. The bottom layer used for waste absorption was then removed, followed by the combination of the second and third layers. Both layers were mounted together firmly through the adhesive surface of the third PVC layer. The amplification reagent was added into the glass fiber on the second layer covered by a disposable tape. The tape-covered zone was then moved into the covered heating compartment of the hand-held heating device for amplification at 65 °C. After the amplification, a denaturation step was performed at 95 °C to separate the double-stranded DNAs into single-stranded DNAs for being hybridized with the AuNP-DP. The second and third layers were then combined firmly with the top layer (lateral flow layer) through the adhesive surface of the third layer. The glass fibers of the first and second layer were then attached together, creating a compact lateral flow strip. The integrated strip was moved into the nonheating compartment holding a disposable micro-centrifuge tube containing SSC buffer for LFA.

Clinical Sample Testing by Using the Integrated Sample-to-Answer LFA. To prove the potential of integrating the optimum fluidic control strategy into our prototype LFA for sensitive sample-to-answer target detection, we tested our prototype with HBV blood clinical sample according to the published protocol.[24] With prior informed written consent, the human blood samples from 16 HBV patients were obtained from the First Affiliated Hospital of Xi'an Jiaotong University. The study was approved by the Institute Research Ethics Committee of The First Affiliated Hospital. The positive blood samples were confirmed by conventional DNA analysis, involving tube-based extraction using Purelink Genomic DNA Mini Kits (Invitrogen), followed by quantitative-real time PCR (qPCR) or tube-based LAMP and electrophoresis according to the manufacturer's instruction. All sequences used were obtained from Sangon Biotechnology Co., Ltd. (Shanghai, China) (Supplementary Table 1). To further confirm the specificity of the assay using our prototype, two clinically confirmed HCV-positive samples, two Cytomegalovirus-positive samples, and three blood samples from healthy donors were also tested with the modified sample-to-answer LFA.

Statistical Analysis. One-way ANOVA with a Tukey posthoc test was used to compare the data among different groups in all assays. Data were expressed as mean ± standard error of the mean of three independent experiments ($n = 3$). $p < 0.05$ was reported as statistically significant.

RESULTS AND DISCUSSION

Sensitivity Enhancement by Incorporating a Glass Fiber Shunt. Generally, there are two ways of reducing the reagent transport rate in paper without modification of strip size. The first way is to incorporate an additional porous medium (e.g., cellulose) to absorb the fluid and thus reduce its flow rate in the paper,[32] while the other way is to create hydrophobic barriers (e.g., wax barrier) to obstruct the regular flow in the paper.[18] In LFAs, we propose that both ways enable analytical sensitivity enhancement by increasing the binding and reaction rates of biomolecules before being captured by the capturing molecules (in this case, streptavidin) (Figure 1).

In fact, various kinds of nitrocellulose membranes with different lengths and capillary flow rates are available in the market, which may contribute to the assay sensitivity. The nitrocellulose membrane used in this study (2.0 cm length with a flow rate of 180 s/4 cm) is commonly used in research institutes and industries, which has been utilized in our previous studies.[9,12,31,33] In the present study, to evaluate the effect produced by the shunt and PDMS barrier, we do not use the nitrocellulose membrane with an even lower capillary flow rate. We also do not modify the length of the membrane as increasing the length may cause more sample or reagent consumption, whereas reducing the length may result in poor sensitivity due to the lower biomolecule interaction rate and shorter time for the biomolecules to reach the test zone.[18]

In an effort toward miniaturization of the sensor with a simple fabrication process, which is compatible with POC applications, the size of the conventional strip is maintained (~6 cm × 2.5 cm), including the size and shape of sample and conjugate pads. Additionally, the unmodified conjugate pad could fix the AuNP-DP deposition site, thus producing a consistent result. Therefore, we added a piece of shunt and PDMS barrier into LFA without modifying the shape and size of the pad. To meet the WHO's ASSURED criteria for POC testing, the great challenge would be achieving a sensitive detection over a short period of time. In fact, the flow rate in paper is significantly dependent on the physical characteristics of paper (e.g., pore size). Therefore, selection of an appropriate material for shunt is essential for effective fluidic control. For this, different types of pads including cellulose (GF-08), glass fiber Fusion 5 (Whatman, Inc., Florham Park, NJ), and borosilicate glass fiber (Pall 8964) were compared in terms of the final analytical sensitivity. We found that Fusion 5 with an average pore size of 10 μm showed a significantly lower analytical sensitivity with a higher sample wicking rate, as indicated by 6.5 ± 0.18 min required to reach the test zone as compared to that of cellulose (10.5 ± 0.2 min) and glass fiber Pall 8964 (8.4 ± 0.1 min), resulting in a shorter interaction time between the target and AuNP-DP and hence lowering the assay sensitivity (Figure S1). Cellulose with a smaller pore size (0.5 μm) showed a significant fluidic delay as compared to fusion 5 and glass fiber Pall 8964. This significant fluidic delay might cause a failure of the considerable amount of AuNP-DP-target to completely wick through the nitrocellulose membrane, resulting in the presence of the residual AuNP-DP or AuNP-DP-target (in red) as observed on the glass fiber (Figure S1).

DOI: 10.1021/acs.analchem.6b00195
Anal. Chem. 2016, 88, 6254−6264

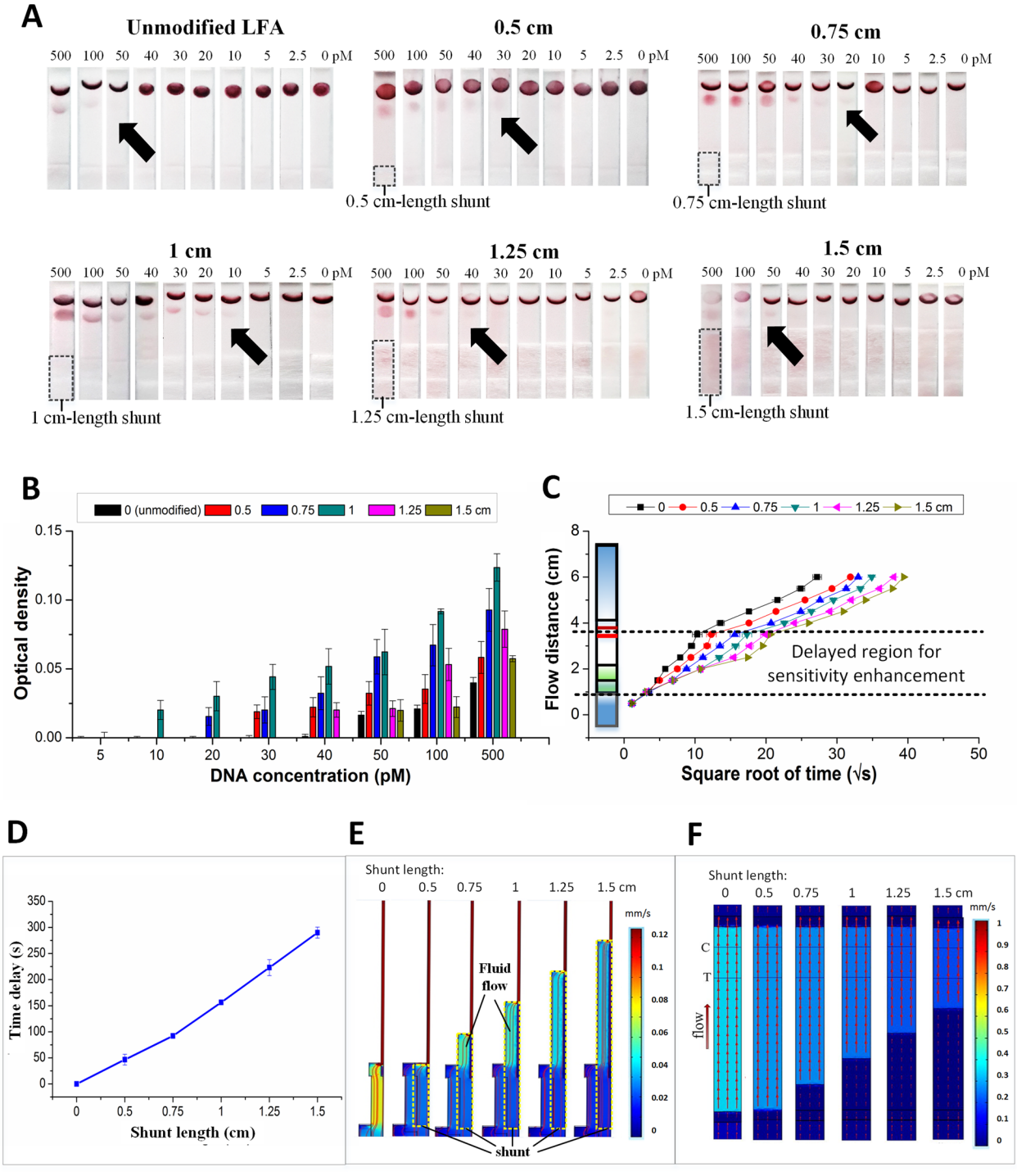

Figure 2. Sensitivity enhancement of LFA by implementation of glass fiber shunt. (A, B) The shunt with the length of 1 cm achieved the highest sensitivity with a detection limit as low as 10 pM, representing 5-fold signal enhancement over unmodified LFA. (C, D) The desirable fluidic delay (156.3 ± 3.36 s) achieved by using 1 cm-length shunt allows optimum interaction of biomolecules, which leads to a significant enhancement in sensitivity of LFA. (E, F) Results of flow velocity simulation of the test strip.

The low amount of AuNP-DP captured by the streptavidin at the test zone results in a significantly lower signal produced in LFA. Unlike cellulose, the glass fiber Pall 8964 with confined pore size (~8 μm) enables all fluid to wick through the shunt and nitrocellulose membrane for target capturing. By reducing the fluid wicking rate, the glass fiber Pall 8964 allows the AuNP-DP and target to have sufficient reaction time before being captured by the streptavidin, hence resulting in a significantly higher ($p < 0.05$) optical density of the test zone (0.263 ± 0.009) as compared to that of fusion 5 (0.171 ± 0.01) and cellulose (0.225 ± 0.01). Therefore, glass fiber Pall 8964 was selected as a material of choice for shunt.

To induce a desirable time delay, which is the duration required for the fluid front to reach the test zone as compared to the unmodified LFA and enhance the sensitivity of LFA, different lengths of shunts (0.5, 0.75, 1, 1.25, 1.5 cm) with the same width to that of lateral flow strip (0.25 cm) were compared (Figure S2A). We do not manipulate the number of

DOI: 10.1021/acs.analchem.6b00195
Anal. Chem. 2016, 88, 6254−6264

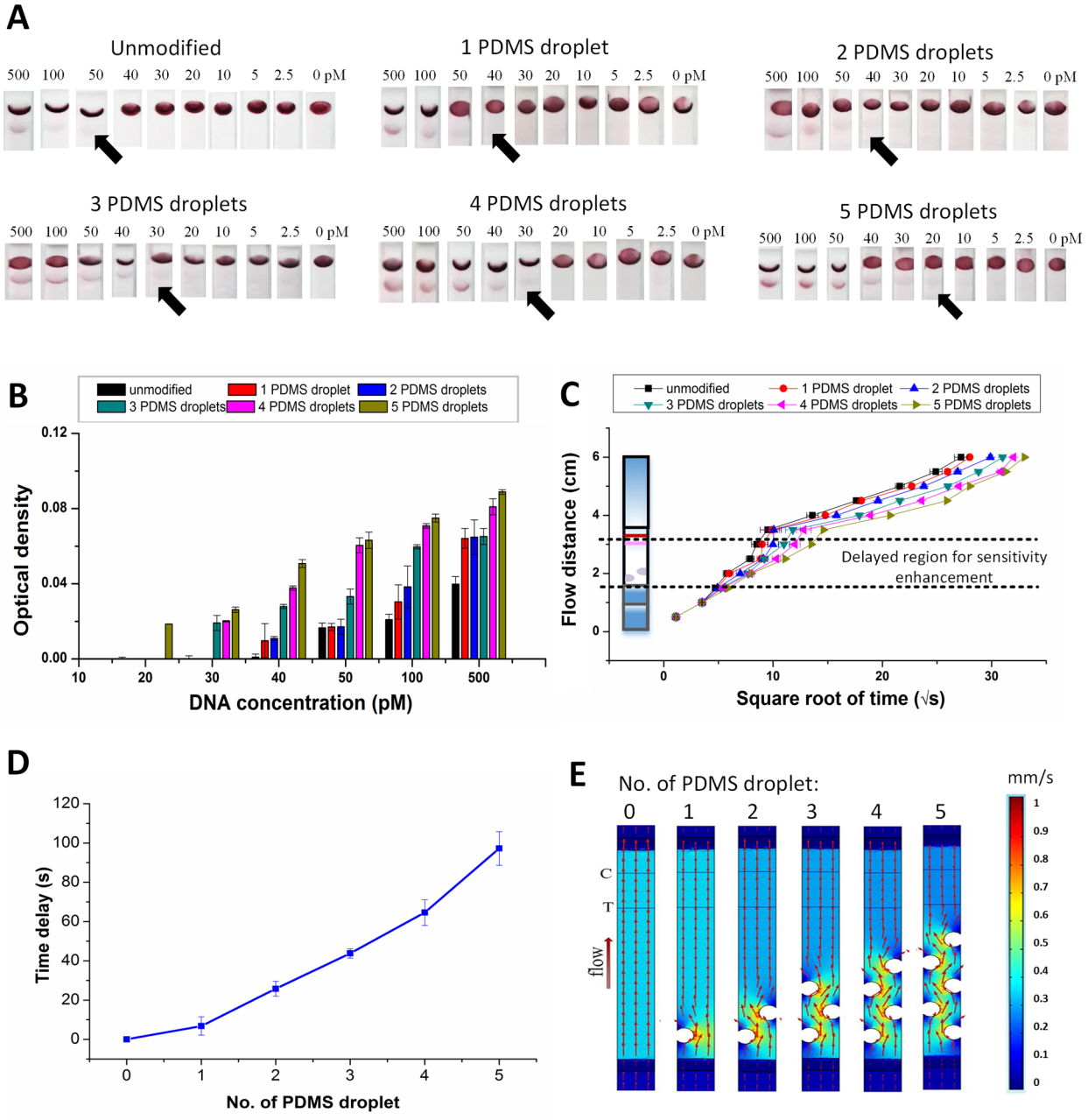

Figure 3. Sensitivity enhancement in LFA by creating PDMS barrier. (A, B) The higher the number of PDMS droplets, the lower is the detection limit achieved as indicated by the detection limit of as low as 20 pM achieved with 5 PDMS droplets. (C, D) The significant fluidic delay was shown with a higher number of PDMS droplets. (E) Results of flow velocity simulation of the test strip.

shunts, to avoid the potential risk of creating gaps between the adjacent layers, which would inconsistently affect the fluid flow. Also, we do not manipulate the shunt thickness, as the glass fiber used in the study is commercially available with limited choice of thickness. The surface area of overlapping region between the sample pad and conjugate pad and that between the conjugate pad and the shunt remained the same (0.5 cm × 0.25 cm). The width of shunt was maintained the same as that of the strip to keep the fabrication process simple. We found that the sensitivity of the assay increased with increasing length of shunt as indicated by the more clearly visible test zone and a significantly lower ($p < 0.05$) detection limit of LFA. For instance, the detection limit for 1 cm-length shunt was 10 pM target DNA, which represents about 5-fold signal enhancement over unmodified LFA (50 pM) (Figure 2A,B). This is basically due to a more desirable time delay produced by the shunts with 1 cm length, as evidenced by 156 ± 3.36 s fluidic delays produced from the shunt region to the test zone as compared to that of the unmodified strip, resulting in an increased interaction rate between the AuNP-DP and target DNA (Figure 2C,D). Theoretically, in the presence of shunt, a significant amount of the fluid from the nitrocellulose membrane is diverted into the shunt, resulting in a reduced flow rate in the nitrocellulose membrane. In the absence of the shunt, the distance moved by the fluid front (L) is described by Washburn's equation,[32] where L is directly proportional to the square root of time ($t^{1/2}$). It was noted that, after reaching the shunt, the absorption of fluid by the shunt reduces the fluid front in the nitrocellulose membrane, as indicated by an increased $t^{1/2}$ (Figure 2E,F).

DOI: 10.1021/acs.analchem.6b00195
Anal. Chem. 2016, 88, 6254−6264

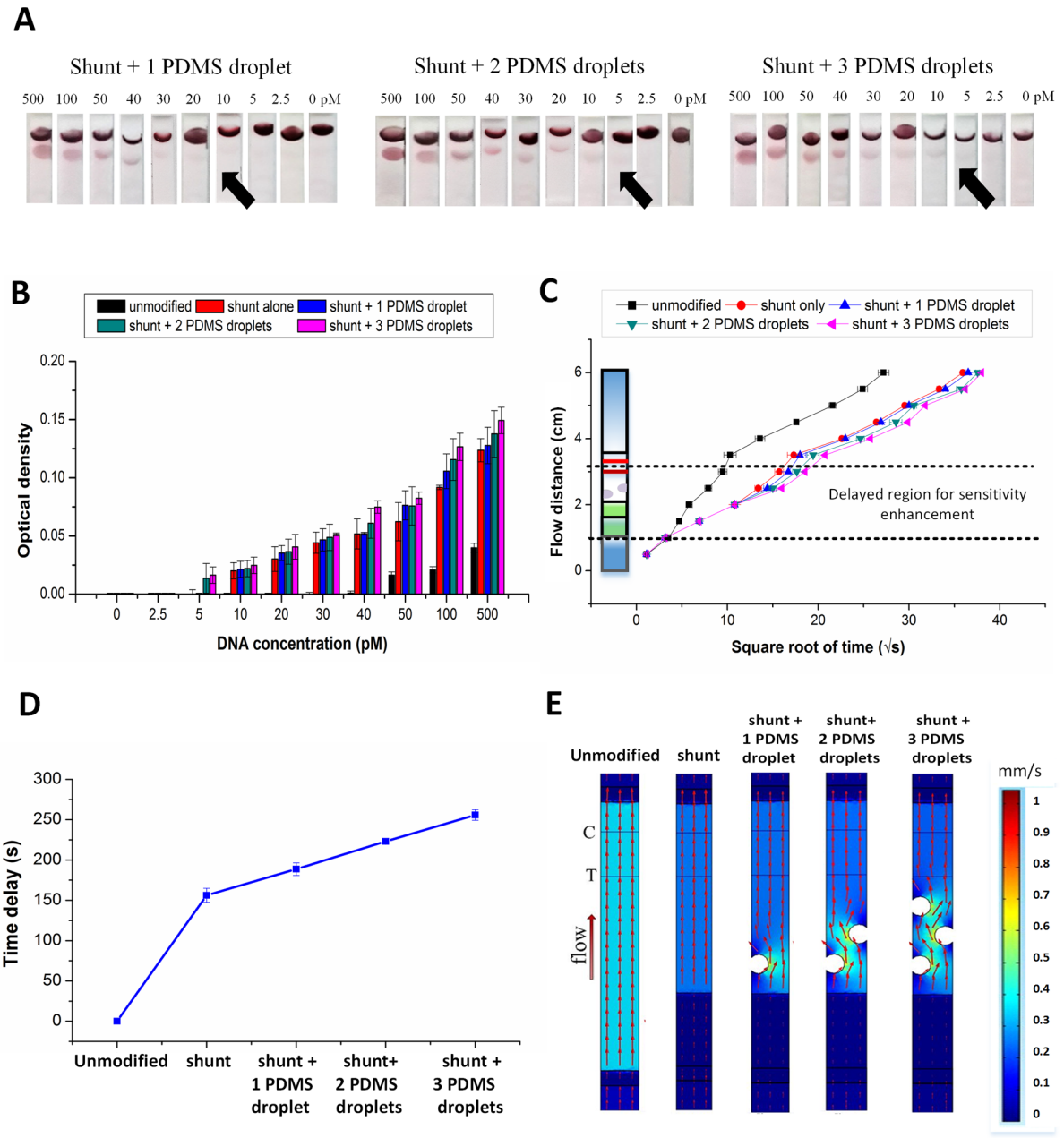

Figure 4. Strategy of combining both glass fiber shunt and PDMS barrier in LFA. (A, B) The optimum of two PDMS droplets in combination with a piece of 1 cm × 2.5 cm shunt achieved a higher sensitivity as indicated by the detection limit as low as 5 pM, representing 10-fold signal enhancement over unmodified LFA. (C, D) The optimum fluidic delay (223.1 ± 2.36 s) achieved by the combination of one shunt and two PDMS droplets significantly enhanced the sensitivity of the assay. (E) Results of flow velocity simulation of the test strip.

However, shunts with a length longer than 1 cm (1.25 and 1.5 cm) had a lower analytical sensitivity (40 and 50 pM, respectively) (Figure 2A,B). This might be due to the higher water absorption capacity (54 μL/cm^2), which results in a failure of the fluid to completely wick through the strip. As a result, a significant amount of AuNP-DP and AuNP-DP-target remains along the glass fiber and nitrocellulose membrane, leading to a significant background signal as compared to the unmodified LFA and shorter-shunt LFA (<1 cm shunt length).

The phenomena of a shunt-induced reduction of fluid velocity were also evaluated using mathematical simulations. For each group, we calculated the average velocity at the test zone. The velocities were calculated to be 0.354, 0.289, 0.272, 0.247, 0.218, and 0.208 mm/s for unmodified LFA and shunts with lengths of 0.5, 0.75, 1.0, 1.25, and 1.5 cm, respectively (Figure S3A). As shown in Figure 2E, the red lines in the shunt indicate the movement of fluid throughout the shunt. This further supports the experimental data, which reveals that the longer the shunt, the larger is the space for biomolecule reaction. Additionally, the longer shunt promotes the flow resistance, which results in the reduction of fluid velocity (Figure 2F) and thus affects the detection sensitivity.

Sensitivity Enhancement by Creating PDMS Barrier. As 5-fold signal enhancement induced by the glass-fiber shunt might not be sufficient for most medical diagnostics, we intended to further improve the analytical sensitivity by creating an additional hydrophobic barrier. As discussed earlier, increasing the length of the shunt showed potential risk of

DOI: 10.1021/acs.analchem.6b00195
Anal. Chem. 2016, 88, 6254−6264

sample loss due to the increased absorbent capacity of the shunt, resulting in a low sensitivity of LFA (Figure 2A,B). Therefore, we suggest that adding a hydrophobic barrier for further sensitivity enhancement would be a better choice, which acts as an obstacle to delay the sample flow without consuming a large volume of sample. To prove the potential of the PDMS barrier to control the fluid flow in LFA, we first performed the LFA by creating a different number of PDMS droplets on the strip without implementing the shunt (Figure S2B).

As our group currently focuses on developing a hand-held apparatus to facilitate both fabrication and operation of the biosensor in remote settings, we performed PDMS dropping, which could be potentially achieved by using a portable apparatus instead of microstructures patterning, which normally requires the benchtop equipment like high-end inkjet printers and electrically powered heaters. In the present study, a hand-held pipet is used to dispense the PDMS onto the nitrocellulose membrane, followed by drying using the prototype hand-held battery-powered heating device. Currently, we are upgrading the functional ball pen previously developed by our group[34] to make it available for direct writing of PDMS on the lateral flow strip, increasing its compatibility with the POC assay. We are also developing a portable PDMS printing device to achieve accurate, precise, and highly reproducible modified lateral flow strips. The entire fabrication and operation process is simple and rapid, which is readily performable in remote settings.

In fact, applying the PDMS onto the nitrocellulose membrane allows the penetration of PDMS into the membrane and creates the hydrophobic zone. To confirm if the PDMS truly acts as a barrier across the nitrocellulose membrane, characterization was performed. SEM reveals the penetration of PDMS droplets into the nitrocellulose membrane, which creates a barrier to obstruct the fluid flow (Figure S4). To determine the effect of the number of PDMS droplets on the sensitivity of LFA, we dropped one, two, three, four, or five drops of PDMS with the volume of 0.1 μL, respectively, onto the nitrocellulose membrane of different groups. Five drops of PDMS are maximal due to the limited space available on the nitrocellulose membrane. We found that increasing PDMS droplets slightly increases the sensitivity of LFA, as indicated by the detection limit of as low as 40, 40, 30, 30, and 20 pM target achieved by one, two, three, four, and five PDMS droplets, respectively (Figure 3A,B). About 2.5-fold signal enhancement was observed in the strip with 5 PDMS droplets over unmodified LFA. We suggest that the sensitivity enhancement might also be associated with the increased biomolecule interaction rate as induced by the fluidic delays, as indicated by the more significant time delay produced by a higher number of PDMS droplets. The time delays were determined by the duration of fluid flow from the region of the first PDMS droplet (from the bottom of the strip) to the test zone, showing 97.2 ± 0.4 s delay produced with 5 PDMS droplets over 6.84 ± 4.7, 25.8 ± 3.8, 43.8 ± 2.36, and 97.2 ± 8.58 s produced with one, two, three, and four droplets, respectively (Figure 3C,D). A similar linear relationship between time delay and the number of barriers is supported by the literature, in which printed baffles were implemented on paper.[35]

The phenomena of PDMS-induced reduction of fluid velocity were also evaluated using mathematical simulations (Figure 3E). The velocities at the test zone were calculated to be 0.354, 0.352, 0.325, 0.296, 0.289, and 0.279 mm/s for unmodified, 1 PDMS droplet, 2 PDMS droplets, 3 PDMS droplets, 4 PDMS droplets, and 5 PDMS droplets, respectively (Figure S3B), indicating that the higher the number of PDMS droplets, the lower is the flow velocity, which is in accordance with our experimental data. It was observed that the PDMS barrier obstructs the fluid flow leading to the different flow magnitude and direction, as indicated by the red arrows shown in Figure 3E. The present results suggest that the higher the number of PDMS droplets, the longer is the nitrocellulose membrane involved in tortuosity. This effect promotes fluid mixing, which could enhance the biomolecule interaction and hence improve the sensitivity of LFA.

Sensitivity Enhancement by a Combination of Glass Fiber Shunt and PDMS Barrier. To demonstrate the potential of combining both shunt and PDMS barrier in LFA for enhancing sensitivity with optimum fluidic control, we determined the number of PDMS droplets required to be combined with the optimum 1 cm length of shunt that would not significantly consume a large volume of reagent or sample (Figure S2C). One, two, or a maximum of three PDMS droplets (due to the limited space available to create PDMS barrier in the presence of shunt) were dropped onto the lateral flow strip. It was found that the detection limits of LFAs were 10, 5, and 5 pM target with one, two, and three PDMS droplets, respectively (Figure 4A,B). Two PDMS droplets could achieve a 10-fold signal enhancement over unmodified LFA, which is again associated with the optimum biomolecule interactions as previously discussed. In contrast, three drops of PDMS creates fluidic delays of 255.8 ± 6.5 s (Figure 4C,D), where there is no significant difference from two drops of PDMS in terms of time delay, thus producing the same detection limit of 5 pM. The phenomena of fluid velocity control by these techniques were also further confirmed using mathematical simulations (Figure 4E). The velocities at the test zone were 0.354, 0.242, 0.228, and 0.221 mm/s for unmodified, combination of shunt with 1 PDMS droplet, combination of shunt with 2 PDMS droplets, and combination of shunt with 3 PDMS droplets, respectively (Figure S3C). This indicates that, with a fixed length of shunt (1 cm), the higher the number of PDMS droplets, the lower is the fluid velocity, which supports the experimental data. In addition, consistent with the data in Figure 3E, a higher number of PDMS droplets leads to a longer nitrocellulose membrane involved in tortuosity (Figure 4E), resulting in higher biomolecule reaction rates and thus a higher signal intensity of the test zone.

In short, the rate of the fluid flow through the lateral flow strip is altered by incorporation of the shunt and the PDMS barrier. In the presence of shunt with the optimum length of 1 cm, a significant amount of the sample from the nitrocellulose membrane is diverted into the shunt, causing a fluidic delay in the nitrocellulose membrane. The shunt acts as a reaction space for AuNP-DP and target DNA, hence increasing their interaction rate. The process results in more formation of AuNP-DP-target complexes, which eventually bind to the streptavidin at the test zone and produce a high intensity of test zone, thus enhancing the analytical sensitivity of the assay. In addition to the shunt, incorporating the optimum two droplets of PDMS induces the tortuosity effects, which obstructs the fluid flow and leads to the different flow magnitude and direction. This effect promotes fluid mixing, which could enhance the AuNP-DP and target DNA interaction, thus further enhancing the sensitivity of LFA. The fluidic control strategy allows highly sensitive target detection, achieving a 10-fold signal enhancement over conventional unmodified LFA.

DOI: 10.1021/acs.analchem.6b00195
Anal. Chem. 2016, 88, 6254−6264

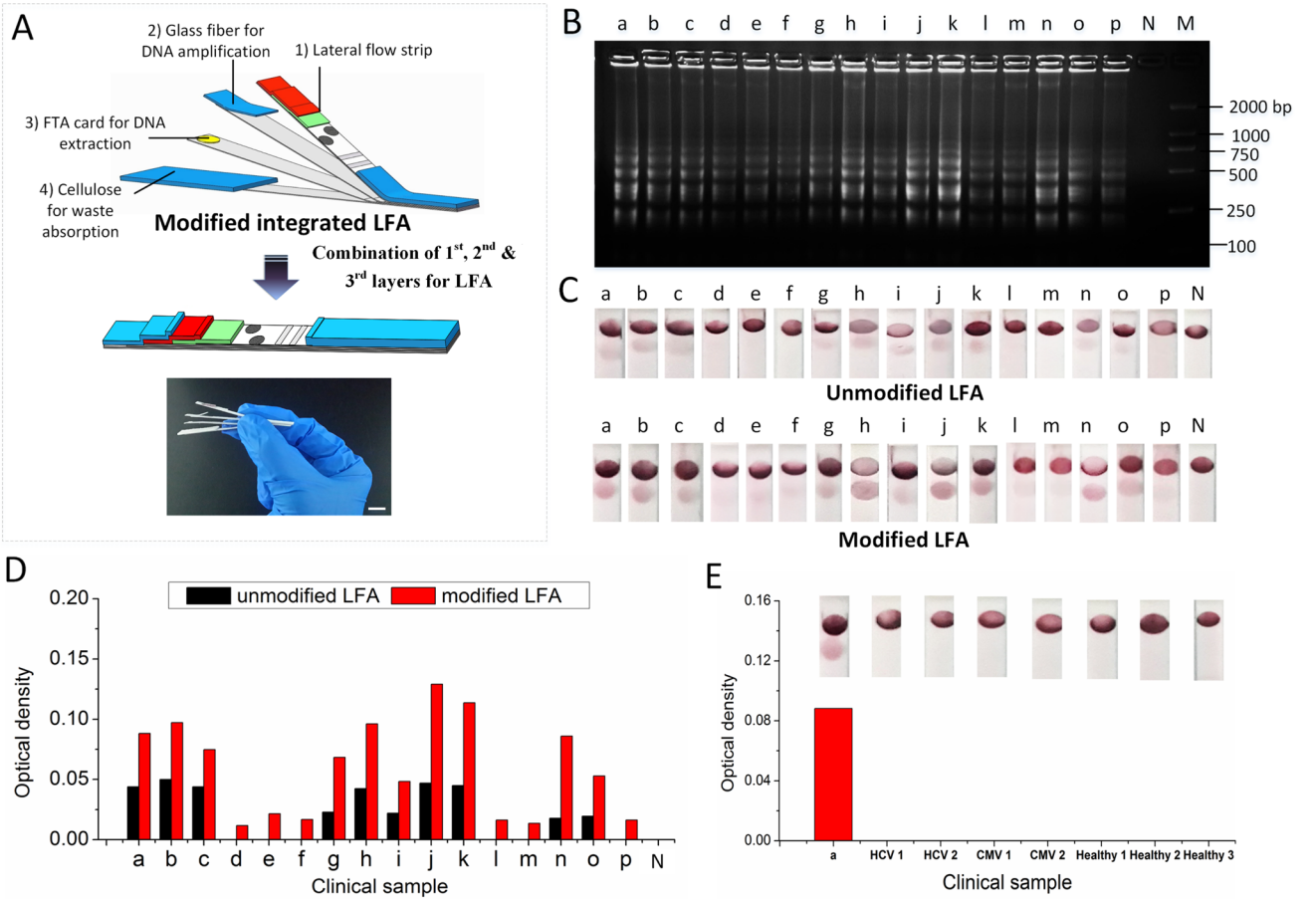

Figure 5. Integration of both sensitivity enhancement techniques into a sample-to-answer LFA for clinical sample testing. (A) A schematic diagram of the modified sample-to-answer LFA for paper-based DNA extraction, amplification, and lateral flow detection (scale bar, 1 cm). In accordance with the result of gold standard qPCR, 16 HBV positive samples (samples a–p) showed clearly visible bands in electrophoresis (B) (N = negative control, M = 100–2000 bp marker). By integrating the fluidic control techniques into our prototype sample-to-answer LFA, it was found that, at high target concentration, a higher intensity of red signal was observed at the test zone in modified LFA as compared to that of unmodified LFA, whereas at low target concentration, the red signal can still be observed in modified LFA but is absent in unmodified LFA (C), which corresponds to the optical densities obtained through gray scale analysis (D). Good specificity was demonstrated by the only positive result shown in HBV sample (sample a) whereas the two HCV samples (HCV 1 and 2), two cytomegalovirus samples (CMV 1 and 2), and three blood samples from healthy donors (Healthy 1, 2, and 3) showed negative results (E).

The proposed modified LFA offers several advantages over the existing fluidic control methods. Unlike the LFAs with implemented temperature-sensitive wax-barriers, incorporating heat-resistant PDMS barrier enables all types of temperature-dependent amplification in NAT. In contrast to the LFA with architecture modifications, the proposed LFA allows an easier manufacturing process and reduces the volume of sample and reagent required. Future work should focus on evaluation of different parameters of the shunt, including different shunt numbers (with different pattern of stacking) and shunt thicknesses (synthetic shunts with different thicknesses) to be compared with that of the shunt length for LFA sensitivity improvement. Future work should also include the development of a portable PDMS printing device to achieve accurate, precise, and highly reproducible lateral flow strips, allowing rapid strip fabrication and sensitive target detection in remote settings.

Integration of Sensitivity Enhancement Techniques into Sample-to-Answer LFA with Clinical Sample Testing. As there is an urgent need for the development of a sample-to-answer LFA for sensitive medical diagnosis in resource-poor settings, we evaluated the potential of integrating the optimum fluidic control strategy into our prototype sample-to-answer LFA (Figure 5A). To prove the potential use of this modified LFA for sensitive clinical diagnosis, Hepatitis B Virus was selected as model analyte in clinical assessment. About 16 HBV-positive clinical samples, which were confirmed by gold standard qPCR (Supplementary Table 2), were initially tested with conventional benchtop DNA analysis, involving tube-based DNA extraction, tube-based LAMP, and electrophoresis. In accordance with the result of gold standard qPCR, electrophoresis showed a clearly visible band with high viral DNA concentration (10^7 to 10^8 IU/mL) and light color of bands with low viral DNA concentration (10^2 to 10^4 IU/mL) (Figure 5B). To demonstrate the potential of the sample-to-answer LFA to sensitively detect HBV, fluidic control techniques were incorporated into our prototype. Interestingly, it was found that testing the patient blood with a high concentration of HBV results in a higher optical density of test zone using the modified sample-to-answer LFA whereas a lower intensity of test zone was observed in the unmodified sample-to-answer LFA. On the other hand, in the presence of a low HBV concentration in blood, modified sample-to-answer LFA showed a lower intensity of test zone whereas unmodified LFA

DOI: 10.1021/acs.analchem.6b00195
Anal. Chem. 2016, 88, 6254–6264

showed no signal at the test zone (Figure 5C,D). Generally, in acute HBV infections, the concentration of HBV could be as low as 10^2 to 10^4 IU/mL.[36,37] Using the modified sample-to-answer LFA, the prototype was able to detect the clinical samples with HBV concentrations of as low as ~10^2 IU/mL, highlighting its potential application in rapid and early detection of HBV infection.

Additionally, the good specificity of the sample-to-answer LFA was also evidenced by the only positive result shown in HBV-positive clinical samples, whereas other samples such as Hepatitis C virus (HCV 1 and 2), cytomegalovirus (CMV 1 and 2), and samples from healthy donors (Healthy 1, 2, and 3) showed negative results (Figure 5E). Unlike the aforementioned conventional method, the modified sample-to-answer LFA enables rapid naked eye detection, which can also be quantified using a smartphone. The entire sample-to-answer process requires only about 1 h instead of 5 h required in conventional tube-based extraction, amplification, and detection methods. Collectively, our modified prototype enables low cost, portable, and rapid sample in-to-answer out detection of target analyte with comparable performance to the conventional laboratory-based DNA analysis. We envision that our current prototype could be broadly applied to other target analytes, offering great potential for a wide range of applications.

CONCLUSION

In the present study, we propose a simple strategy of integrating paper-based shunt and PDMS barrier into the lateral flow strip. With an optimum size of the shunt and number of PDMS droplets, the fluidic transport can be greatly controlled in LFA without consuming a large volume of sample. The phenomena of fluidic delay, which contributes to the sensitivity enhancement, were evaluated by the mathematical simulation, through which we found the fluid movement throughout the shunt and the tortuosity effects in the presence of PDMS. This fluidic control strategy allows highly sensitive medical diagnosis, resulting in 10-fold signal enhancement over conventional unmodified LFA. Additionally, integrating this strategy into a prototype sample-to-answer LFA enables highly sensitive detection of HBV (~10^2 IU/mL), which is comparable to the conventional laboratory-based assays. The proposed modified sample-to-answer LFA shows great promise to sensitively detect various target analytes for a broad range of applications in the near future.

ASSOCIATED CONTENT

Supporting Information

The Supporting Information is available free of charge on the ACS Publications website at DOI: 10.1021/acs.analchem.6b00195.

Selection of an appropriate shunt material; schematic of modified lateral flow strips; the average velocity at the test zone; characterization of LFA incorporated with PDMS barrier; oligonucleotide sequences used in the study; HBV-positive clinical samples confirmed by qPCR (PDF)

AUTHOR INFORMATION

Corresponding Author

*E-mail: fengxu@mail.xjtu.edu.cn.

Notes

The authors declare no competing financial interest.

ACKNOWLEDGMENTS

This work was financially supported by the Major International Joint Research Program of China (11120101002), the International Science & Technology Cooperation Program of China (2013DFG02930), the Postgraduate Research Grant (PPP) and the UM High Impact Research Grant UM-MOHE (UM.C/HIR/MOHE/ENG/44) from the Ministry of Higher Education Malaysia. H.R. would like to acknowledge the National Natural Science Foundation of China (81302029), Natural Science Foundation of Shaanxi Province of China (2014JQ4149), Fundamental Research Funds for the Central Universities in Xi'an Jiaotong University (xjj2015086), and China Postdoctoral Science Foundation (2015M570841). This work was performed at the Bioinspired Engineering and Biomechanics Center (BEBC) at Xi'an Jiaotong University.

REFERENCES

(1) Katsanis, S. H.; Katsanis, N. *Nat. Rev. Genet.* **2013**, *14*, 415−426.
(2) Akhtar, A.; Fuchs, E.; Mitchison, T.; Shaw, R. J.; St Johnston, D.; Strasser, A.; Taylor, S.; Walczak, C.; Zerial, M. *Nat. Rev. Mol. Cell Biol.* **2011**, *12*, 669−674.
(3) Krebs, M. G.; Metcalf, R. L.; Carter, L.; Brady, G.; Blackhall, F. H.; Dive, C. *Nat. Rev. Clin. Oncol.* **2014**, *11*, 129−144.
(4) Martinez, A. W.; Phillips, S. T.; Whitesides, G. M.; Carrilho, E. *Anal. Chem.* **2010**, *82*, 3−10.
(5) Wang, J. H.; Wang, C. H.; Lee, G. B. *Ann. Biomed. Eng.* **2012**, *40*, 1367−1383.
(6) Wang, S.; Xu, F.; Demirci, U. *Biotechnol. Adv.* **2010**, *28*, 770−781.
(7) Feng, S.; Choi, J. R.; Lu, T. J.; Xu, F. *Adv. Porous Flow* **2015**, *5*, 16−29.
(8) Choi, J. R.; Hu, J.; Feng, S.; Wan Abas, W. A. B.; Pingguan-Murphy, B.; Xu, F. *Biosens. Bioelectron.* **2016**, *79*, 98.
(9) Tang, R.; Yang, H.; Choi, J. R.; Gong, Y.; Hu, J.; Feng, S.; Pingguan-Murphy, B.; Mei, Q.; Xu, F. *Talanta* **2016**, *152*, 269−276.
(10) Choi, J.; Hu, J.; Wang, S.; Yang, H.; Wan Abas, W. A. B.; Pingguan-Murphy, B.; Xu, F. *Crit. Rev. Biotechnol.* **2016**, 1.
(11) Choi, J. R.; Hu, J.; Gong, Y.; Feng, S.; Wan Abas, W. A. B.; Pingguan-Murphy, B.; Xu, F. *Analyst* **2016**, DOI: 10.1039/C5AN02532J.
(12) Choi, J. R.; Hu, J.; Feng, S.; Wan Abas, W. A. B.; Pingguan-Murphy, B.; Xu, F. *Biosens. Bioelectron.* **2016**, *79*, 98−107.
(13) He, Y.; Zhang, S.; Zhang, X.; Baloda, M.; Gurung, A. S.; Xu, H.; Zhang, X.; Liu, G. *Biosens. Bioelectron.* **2011**, *26*, 2018−2024.
(14) Baeumner, A. J.; Cohen, R. N.; Miksic, V.; Min, J. *Biosens. Bioelectron.* **2003**, *18*, 405−413.
(15) Moghadam, B. Y.; Connelly, K. T.; Posner, J. D. *Anal. Chem.* **2015**, *87*, 1009−1017.
(16) Chiu, R. Y.; Jue, E.; Yip, A. T.; Berg, A. R.; Wang, S. J.; Kivnick, A. R.; Nguyen, P. T.; Kamei, D. T. *Lab Chip* **2014**, *14*, 3021−3028.
(17) Qin, Z.; Chan, W. C.; Boulware, D. R.; Akkin, T.; Butler, E. K.; Bischof, J. C. *Angew. Chem., Int. Ed.* **2012**, *51*, 4358−4361.
(18) Rivas, L.; Medina-Sánchez, M.; de la Escosura-Muñiz, A.; Merkoçi, A. *Lab Chip* **2014**, *14*, 4406−4414.
(19) Parolo, C.; Medina-Sanchez, M.; de la Escosura-Muniz, A.; Merkoci, A. *Lab Chip* **2013**, *13*, 386−390.
(20) Choi, S.; Lee, J.-H.; Kwak, B. S.; Kim, Y. W.; Lee, J. S.; Choi, J.-S.; Jung, H.-I. *BioChip J.* **2015**, *9*, 116−123.
(21) Choi, J. R.; Tang, R.; Wang, S.; Wan Abas, W. A. B.; Pingguan-Murphy, B.; Xu, F. *Biosens. Bioelectron.* **2015**, *74*, 427.
(22) Xu, Z.; Zhao, Y.; Dai, L.; Lin, T. *Particle & Particle Systems Characterization* **2014**, *31*, 839−842.
(23) Choi, H.; Im, K.; Chang, T. *Macromol. Res.* **2012**, *20*, 101−105.
(24) Zaytseva, N. V.; Montagna, R. A.; Baeumner, A. J. *Anal. Chem.* **2005**, *77*, 7520−7527.

DOI: 10.1021/acs.analchem.6b00195
Anal. Chem. 2016, 88, 6254−6264

(25) Glynou, K.; Ioannou, P. C.; Christopoulos, T. K.; Syriopoulou, V. *Anal. Chem.* **2003**, *75*, 4155−4160.
(26) Martinez, A. W.; Phillips, S. T.; Whitesides, G. M. *Proc. Natl. Acad. Sci. U. S. A.* **2008**, *105*, 19606−19611.
(27) Liu, H.; Patil, P.; Narusawa, U. *Entropy* **2007**, *9*, 118.
(28) Liu, Z.; Hu, J.; Zhao, Y.; Qu, Z.; Xu, F. *Appl. Therm. Eng.* **2015**, *88*, 280−287.
(29) Brooks, C. S.; Purcell, W. R. *Petroleum Transactions, AIME* **1952**, 289−296.
(30) Parolo, C.; Medina-Sánchez, M.; de la Escosura-Muñiz, A.; Merkoçi, A. *Lab Chip* **2013**, *13*, 386−390.
(31) Choi, J. R.; Hu, J.; Tang, R.; Gong, Y.; Feng, S.; Ren, H.; Wen, T.; Li, X.; Wan Abas, W. A. B.; Pingguan-Murphy, B.; et al. *Lab Chip* **2016**, *16*, 611.
(32) Toley, B. J.; McKenzie, B.; Liang, T.; Buser, J. R.; Yager, P.; Fu, E. *Anal. Chem.* **2013**, *85*, 11545−11552.
(33) Hu, J.; Wang, L.; Li, F.; Han, Y. L.; Lin, M.; Lu, T. J.; Xu, F. *Lab Chip* **2013**, *13*, 4352−4357.
(34) Li, Z.; Li, F.; Hu, J.; Wee, W.; Han, Y.; Pingguan-Murphy, B.; Lu, T.; Xu, F. *Analyst* **2015**, *140*, 5526.
(35) Apilux, A.; Ukita, Y.; Chikae, M.; Chailapakul, O.; Takamura, Y. *Lab Chip* **2013**, *13*, 126−135.
(36) Gong, M. M.; Nosrati, R.; San Gabriel, M. C.; Zini, A.; Sinton, D. *J. Am. Chem. Soc.* **2015**, *137*, 13913−13919.
(37) Rehermann, B.; Nascimbeni, M. *Nat. Rev. Immunol.* **2005**, *5*, 215−229.

DOI: 10.1021/acs.analchem.6b00195
Anal. Chem. 2016, 88, 6254−6264